

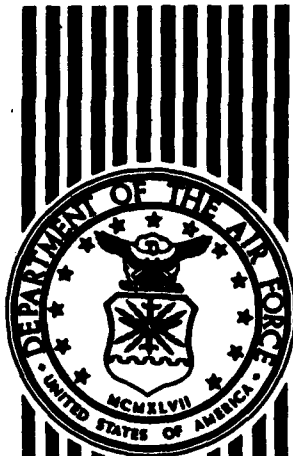
AD-A243 170



DTIC
ELECTE
DEC 2 1991
S C D

1

ESL-TR-88-71



CID SPECTRA OF SELECTED TARGET MOLECULES

R.I. MARTINEZ

NATIONAL BUREAU OF STANDARDS
CENTER FOR CHEMICAL PHYSICS
GAITHERSBURG MD 20879

DECEMBER 1989

FINAL REPORT

JULY 1984 - SEPTEMBER 1987

APPROVED FOR PUBLIC RELEASE: DISTRIBUTION UNLIMITED

91-16567



AIR FORCE ENGINEERING & SERVICES CENTER
ENGINEERING & SERVICES LABORATORY
TYNDALL AIR FORCE BASE, FLORIDA 32403

91 1126 055

NOTICE

PLEASE DO NOT REQUEST COPIES OF THIS REPORT FROM
HQ AFESC/RD (ENGINEERING AND SERVICES LABORATORY).

ADDITIONAL COPIES MAY BE PURCHASED FROM:

NATIONAL TECHNICAL INFORMATION SERVICE
5285 PORT ROYAL ROAD
SPRINGFIELD, VIRGINIA 22161

FEDERAL GOVERNMENT AGENCIES AND THEIR CONTRACTORS
REGISTERED WITH DEFENSE TECHNICAL INFORMATION CENTER
SHOULD DIRECT REQUESTS FOR COPIES OF THIS REPORT TO:

DEFENSE TECHNICAL INFORMATION CENTER
CAMERON STATION
ALEXANDRIA, VIRGINIA 22314

UNCLASSIFIED

SECURITY CLASSIFICATION OF THIS PAGE

Form Approved
OMB No. 0704-0188

REPORT DOCUMENTATION PAGE

1a. REPORT SECURITY CLASSIFICATION			1b. RESTRICTIVE MARKINGS			
2a. SECURITY CLASSIFICATION AUTHORITY			3. DISTRIBUTION/AVAILABILITY OF REPORT			
2b. DECLASSIFICATION/DOWNGRADING SCHEDULE			Approved for Public Release Distribution Unlimited			
4. PERFORMING ORGANIZATION REPORT NUMBER(S)			5. MONITORING ORGANIZATION REPORT NUMBER(S)			
			ESL-TR-88-71			
6a. NAME OF PERFORMING ORGANIZATION National Bureau of Standards Center for Chemical Physics		6b. OFFICE SYMBOL (if applicable)	7a. NAME OF MONITORING ORGANIZATION Air Force Engineering and Services Center			
6c. ADDRESS (City, State, and ZIP Code) Gaithersburg MD 20879		7b. ADDRESS (City, State, and ZIP Code) HQ AFESC/RDVS Tyndall AFB FL 32403				
8a. NAME OF FUNDING / SPONSORING ORGANIZATION HQ AFESC		8b. OFFICE SYMBOL (if applicable) RDV	9. PROCUREMENT INSTRUMENT IDENTIFICATION NUMBER MIPR N84-56; MIPR N84-56 A01 MIPR N85-22; MIPR N86-12; MIPR N87-12			
8c. ADDRESS (City, State, and ZIP Code) Tyndall AFB FL 32403-6001			10. SOURCE OF FUNDING NUMBERS			
PROGRAM ELEMENT NO.		PROJECT NO.	TASK NO.	WORK UNIT ACCESSION NO.		
0100		83	11	08		
11. TITLE (Include Security Classification) CID Spectra of Selected Target Molecules (U)						
12. PERSONAL AUTHOR(S) R. I. Martinez						
13a. TYPE OF REPORT Final		13b. TIME COVERED FROM Jul 84 to Sep 87		14. DATE OF REPORT (Year, Month, Day) December 1989	15. PAGE COUNT 41	
16. SUPPLEMENTARY NOTATION Availability of this report is specified on reverse of the front cover						
17. COSATI CODES			18. SUBJECT TERMS (Continue on reverse if necessary and identify by block number)			
FIELD	GROUP	SUB-GROUP	Collisionally Induced Dissociation, Mass Spectrometry Tandem Quadrupole			
19. ABSTRACT (Continue on reverse if necessary and identify by block number)						
This technical report described research into the molecular dynamics of the collisionally induced dissociation (CID) process. This process occurs in tandem mass spectrometers, and is the major process by which primary or parent ions are converted into daughter ions of smaller mass. This work was undertaken in search of a means of standardizing conditions for tandem mass spectrometers so that standard spectral libraries could be collected and used to identify environmental unknowns. This research indicates that CID cross sections for the parent ions can be reproducibly measured as a function of collision energy, and are characteristic of the parent ion structures. Measurement of CID cross sections offers a new means of identifying unknown compounds.						
20. DISTRIBUTION/AVAILABILITY OF ABSTRACT <input checked="" type="checkbox"/> UNCLASSIFIED/UNLIMITED <input type="checkbox"/> SAME AS RPT. <input type="checkbox"/> DTIC USERS			21. ABSTRACT SECURITY CLASSIFICATION UNCLASSIFIED			
22a. NAME OF RESPONSIBLE INDIVIDUAL Howard T. Mayfield, GS-12			22b. TELEPHONE (Include Area Code) 904-283-4298	22c. OFFICE SYMBOL HQ AFESC/RDVS		

SUMMARY

The primary objective of this research program is to elucidate the molecular dynamics within tandem mass spectrometers (MS/MS). This knowledge base is essential to the successful development of a generic MS/MS database. This report provides an analysis of the various kinetic and instrument parameters (and the complex interplay among them) which influence the spectra observed in tandem mass spectrometers. The focus of the discussion is the set of conditions which would have to be satisfied in order to generate instrument-independent spectra. Also discussed is the form a generic MS/MS database could take. Experimental results validate the concepts discussed.

Accession For	
NTIS ORAI	<input checked="" type="checkbox"/>
DTIC TAB	<input type="checkbox"/>
Unannounced	<input type="checkbox"/>
Justification	
By	
Distribution/	
Availability Codes	
Dist	Avail and/or Special
A-1	



PREFACE

This report was prepared by the Center for Chemical Physics, National Institute of Standards and Technology (formerly National Bureau of Standards), Gaithersburg MD 20899, under MIPR Numbers N84-56, N85-22, N86-18, and N87-12, for the Air Force Engineering and Services Center, Engineering and Services Laboratory (AFESC), Tyndall Air Force Base FL.

This report summarized work performed between July 1984 and September 1987.

This report has been reviewed by the Public Affairs Office (PA) and is releasable to the National Technical Information Service (NTIS). At NTIS, it will be available to the general public, including foreign nationals.

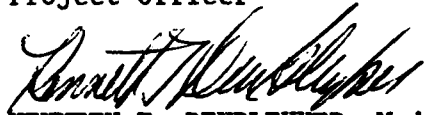
This technical report has been reviewed and is approved for publication.



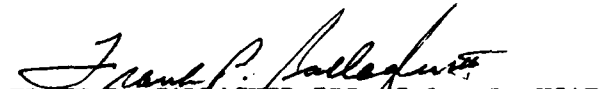
HOWARD T. MAYFIELD, GS-12
Project Officer



F. THOMAS LUBOZYNSKI, Major, USAF, BSC
Chief, Environics Division



KENNETH T. DENBLEYKER, Major, USAF
Chief, Environmental Sciences Branch



FRANK P. GALLAGHER III, Colonel, USAF
Director, Engineering and Services
Laboratory

TABLE OF CONTENTS

Section	Title	Page
I	INTRODUCTION	1
	A. OBJECTIVE	1
	B. BACKGROUND	1
	C. SCOPE	2
II	DYNAMICAL PREREQUISITES	5
III	KEY MS/MS PARAMETERS	7
IV	ENERGY DEPENDENCE OF CAD SPECTRA	10
	A. SINGLE COLLISIONS	10
	B. MULTIPLE COLLISIONS	11
	C. E_{cm}	12
V	REACTION-INDUCED MASS DISCRIMINATION	13
VI	GENERIC MS/MS DATABASE	15
VII	EXPERIMENTAL VALIDATION	19
	A. EXPERIMENTAL PROTOCOL	20
	B. RESULTS	26
	C. DISCUSSION	29
VIII	ROUND ROBIN FOR XQQ INSTRUMENTS	31
IX	CONCLUSIONS AND RECOMMENDATIONS	32
	A. CONCLUSIONS	32
	B. RECOMMENDATIONS	33
	REFERENCES	34
APPENDIX		
A	ASMS WORKSHOP REPORT	39

LIST OF FIGURES

Figure	Title	Page
1	Schematic of NBS QQQ Instrument. EIV, EXT, L1-L5, etc., are Ion Optical Lens Elements.	21
2	Plots of (a) $\ln Y$ vs. SF_6 Target Pressure P for $E_{coll} = 40$ eV (LAB) and (b) of σ vs. E_{cm}	27
3	Plots of $\ln W_i$ ($i = \alpha$ to δ) vs. SF_6 Target Pressure P for $E_{coll} = 40$ eV (LAB).	28

GLOSSARY OF TERMS

Close-Coupled Design - A QQQ instrument which uses closely coupled rf quadrupole fields throughout. The ions never leave the quadrupole field during their flight path. This minimizes ion losses due to defocussing as ions pass through the fringing fields between quadrupoles. It reduces the possibility of mass-dependent lens-focusing effects between quadrupoles. (See References 8-10 for a detailed discussion.)

Collisionally Activated Dissociation - The fragmentation observed subsequent to an $A^+ + B$ interaction wherein the A^+ is activated by translational-to-internal energy conversion (the ionic fragments are characteristic of the A^+ ion).

Collision Induced Dissociation - Same as Collisionally Activated Dissociation.

Dynamically Correct - See Section II.

Key MS/MS Parameters - See Section III.

MS/MS - Tandem mass spectrometry within XQQ instruments (QQQ, BEQQ hybrid, etc.) is used for the analysis of multicomponent mixtures. The analysis makes use of the CAD of "parent" ions. A "parent" ion may be a molecular radical cation, a protonated molecule, or a "progeny" fragment ion (daughter, granddaughter, etc. produced by the CAD of a larger precursor parent ion). A "parent" ion selected by X1 interacts with a target gas within Q2. Q2 channels undissociated "parent" ions and "progeny" fragment ions into Q3. The instrument thus produces a CAD spectrum of each initially-selected "parent" ion.

Parent/Progeny Ions - See MS/MS above.

Reaction-Induced Fragmentation - The fragmentation observed subsequent to an $A^+ + B$ interaction which produces a transient adduct AB^+ which is not stabilized (the ionic fragments are characteristic of the transient AB^+ adduct ion).

Reaction-Induced "Mass Discrimination" - See Section V.

Restrictive Interquadrupole Apertures - Apertures of diameter $< 1.4 r_0$. (See Reference 8 for a detailed discussion.)

Target Thickness - [B]L; see Section I.

XQQ Instruments - XQQ instruments have three components: X1 Q2 Q3. X1 is the first mass analyzer. X1 can be a quadrupole mass filter (represented by a Q), a reversed-geometry magnetic/electrostatic sector instrument (represented by BE), etc. Q2 is an rf-only quadrupole mass filter. Q3 is the second mass analyzer, a quadrupole mass filter.

LIST OF ABBREVIATIONS, ACRONYMS, AND SYMBOLS

(B)L	See <u>Target Thickness</u> in Glossary.
CAD	Collisionally activated dissociation (see Glossary).
CID	Collision induced dissociation (same as CAD; see Glossary).
E	Collision or interaction energy.
E_{cm}	Center-of-mass interaction energy.
F	The Q2 rf frequency (in MHz).
L	Pathlength.
$\left. \begin{array}{l} L_n W \\ L_n W \\ L_n W \end{array} \right\}$	Defined by Equations (2)-(4)
$L_n Y$	Defined by Equation (1).
MS/MS	Tandem mass spectrometer or tandem mass spectrometry. See <u>MS/MS</u> and <u>XQQ Instruments</u> in Glossary.
Q2	See <u>XQQ Instruments</u> in Glossary.
Q3	See <u>XQQ Instruments</u> in Glossary.
r_0	The Q2 field radius (in cm).
RIF	Reaction-Induced Fragmentation (see Glossary).
XQQ	See <u>XQQ Instruments</u> in Glossary.
α -e	Branching ratios for various reaction channels; see Section I.
σ	Reaction cross section; see Section I.

SECTION I INTRODUCTION

A. OBJECTIVE

There is a need for a generic, instrument-independent database (library) for tandem mass spectrometry (MS/MS) to enable the use and exchange of standardized spectral data among XQQ instruments. XQQ instruments have three components: X1 Q2 Q3. X1 is the first mass analyzer. X1 can be a quadrupole mass filter (represented by a Q), a reversed-geometry magnetic/electrostatic sector instrument (represented by BE), etc. Q2 is an rf-only quadrupole mass filter. Q3 is the second mass analyzer, a quadrupole mass filter.

The objective of this research program is to elucidate the molecular dynamics within XQQ tandem mass spectrometers. This knowledge base is essential to the successful development of a generic MS/MS database. One goal, therefore, is to provide a critical analysis of the effect of various MS/MS parameters on the observed spectra (References 1-12).

B. BACKGROUND

Tandem mass spectrometry within XQQ instruments (QQQ, BEQQ hybrid, etc.) is used for the analysis of multicomponent mixtures (Reference 4). The analysis makes use of the collisionally activated dissociation (CAD) of "parent" ions. A "parent" ion may be a molecular radical cation, a protonated molecule, or a "progeny" fragment ion (daughter, granddaughter, etc. produced by the CAD of a larger precursor parent ion). A "parent" ion selected by X1 interacts with a target gas within Q2. Q2 channels undissociated "parent" ions and "progeny" fragment ions into Q3. The instrument thus, produces a CAD spectrum of each initially selected "parent" ion.

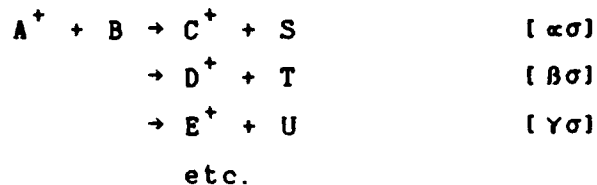
However, XQQ instruments are complex ion-optical devices (References 5-11). Therefore, the choice of parameter settings and/or of instrument design can provide a distorted view of the molecular dynamics of the CAD process [e.g., if there are scattering losses from poor ion containment within Q2, fringing fields between Q2/Q3, etc. (References 5-11)]. Consequently, one observes instrument-dependent CAD spectra.

This was clearly demonstrated in an international round robin (Reference 12) wherein very different CAD spectra were observed for the same molecule. That is, the relative intensities measured in different QQQ instruments for any given pair of progeny ions differed by factors ranging into the hundreds, even though the same nominal operating conditions were supposedly used in each of the QQQ instruments. Therefore, a CAD spectrum of a given species in one XQQ instrument presently cannot be used to identify and quantitate that same species in a different XQQ instrument. Each instrument must have its own calibration curve (ion intensity vs. species concentration) for any one species.

C. SCOPE

This report analyzes the various kinetic and instrument parameters (and the complex interplay among them) which influence the spectra observed in XQQ tandem mass spectrometers. The focus is on the set of conditions which would have to be satisfied to generate instrument-independent spectra. Also discussed is the form such a generic MS/MS database could take.

The discussion will deal with CAD and with reactive systems [i.e., adduct formation, reaction-induced fragmentation (RIF), etc.] under single-collision conditions. CAD and RIF are equally well represented by the following reaction sequence.



Here σ is the total cross section for the $A^+ + B$ interaction at a given collision energy E . Hence, the sum of the cross sections $\alpha\sigma$, $\beta\sigma$, etc. for the individual product channels is $\alpha\sigma + \beta\sigma + \gamma\sigma + \dots = \sigma$. That is, the sum of the branching ratios $\alpha + \beta + \gamma + \dots$ is equal to 1.

The kinetic relations (1)-(4) are applicable under pseudo-first-order ($[B]_0 \gg [A^+]_0$), single-collision conditions for a reaction zone of length L wherein the number density of the target gas is $[B]$ and the "target thickness" is $[B]L$. Note that Equations (1)-(4) can be used under single-collision conditions to describe CAD or RIF subsequent to adduct formation (References 1-3). Thus, C^+ , D^+ , etc. can signify fragments from CAD or RIF. Equation (2) [with $\alpha=1$] can also be used to describe stabilized adduct formation if C^+ is the sole product of the $A^+ + B$ interaction.

$$\ln Y \equiv \ln ([A^+]_0 / [A^+]) = \sigma[B]L \quad (1)$$

and

$$\left. \begin{array}{l}
[C^+] = \alpha[A^+]_0(1 - e^{-\sigma[B]L}) \\
[D^+] = \beta[A^+]_0(1 - e^{-\sigma[B]L}) \\
[E^+] = \gamma[A^+]_0(1 - e^{-\sigma[B]L})
\end{array} \right\} \begin{array}{l}
[D^+]/[C^+] = \beta/\alpha \\
[E^+]/[C^+] = \gamma/\alpha
\end{array}$$

etc., whence

$$\ln W_\alpha \equiv \ln (\alpha[A^+]_0 / (\alpha[A^+]_0 - [C^+])) = \sigma[B]L \quad (2)$$

$$\ln W_\beta \equiv \ln (\beta[A^+]_0 / (\beta[A^+]_0 - [D^+])) = \sigma[B]L \quad (3)$$

$$\ln W_\gamma \equiv \ln (\gamma[A^+]_0 / (\gamma[A^+]_0 - [E^+])) = \sigma[B]L \quad (4)$$

etc.

Note that for $\sigma[B]L \leq 0.2$ ("thin-target" conditions),

$$[C^+]/[A^+]_0 \approx \alpha \sigma[B]L$$

$$[D^+]/[A^+]_0 \approx \beta \sigma[B]L$$

$$[E^+]/[A^+]_0 \approx \gamma \sigma[B]L$$

etc.

Therefore, plots of $[C^+]/[A^+]_0$ vs. $\sigma[B]L$, $[D^+]/[A^+]_0$ vs. $\sigma[B]L$, etc. can provide initial estimates for α , β , etc. once $\sigma[B]L$ has been determined from Equation (1).

In the context of Equations (1)-(4) the instrument-independent CAD spectrum for a given parent ion A^+ in the presence of the CAD gas B would consist of the parent ion signal $[A^+]$ together with the intensities $[C^+]$, $[D^+]$, etc. for each of its progeny ions C^+ , D^+ , etc. Hence, if one knows the dependence of σ , α , β , etc. on the collision energy E, one can reproduce the CAD spectrum of each parent ion A^+ for any given target thickness $[B]L$ within the single-collision regime.

SECTION II DYNAMICAL PREREQUISITES

To obtain standardized instrument-independent CAD spectra, one must make appropriate corrections for ion-optical effects within each XQQ structure. To do so, one must provide a dynamically correct basis for selecting within each XQQ instrument the appropriate settings for the key MS/MS parameters (discussed in Section III).

The reactivity (kinetics) of a molecular system is an intrinsic, generic, and thus transferable property of that system. Therefore, the kinetics (reaction mechanisms and rate coefficients) of selected ion-molecule reactions can be used as molecular probes to determine which combination of key MS/MS parameters provide instrument-independent (dynamically correct) branching ratios for the CAD of polyatomic ions.

The kinetic relations (1)-(4) place severe constraints on the selection of the key MS/MS parameter settings. For σ derived from Equation (1) to equal the σ from Equations (2)-(4) with $\alpha + \beta + \gamma + \delta + \dots = 1$, one must have $[A^+]_0 = [A^+] + [C^+] + [D^+] + [E^+] + \dots$ for any [B] at each interaction energy E. These constraints require that:

1. each product ion be formed only by the primary reaction (no secondary sources; single-collision conditions must prevail),
2. all ions be detected with equal sensitivity (conversion gain corrections for each detector are required for all product ions),
3. there be no scattering losses because of unreactive collisions between ions and the target gas (must have high ion containment within Q2; 100 Percent collection efficiency for product ions and unreacted projectiles),

4. corrections be applied for each product ion for differences in ion containment (transmission) within the Q2Q3 structure.

In principle, one can readily comply with constraints 1. and 2. To comply with constraints 3. and 4., however, the XQQ instrument must have a dynamically correct design. That is, the design should make it possible to adequately control the key MS/MS parameters to provide an undistorted (unbiased) representation of the reaction dynamics (i.e., dynamically correct branching ratios α -6, etc., no back reactions, no scattering losses, minimal fringing fields, no mass discrimination, well-defined gas target, etc.). Instrument designs which are incompatible with these requirements cannot provide dynamically correct performance. Dynamically correct XQQ instruments must be used if one is to develop and use a generic, instrument-independent MS/MS database (see also Section VI).

To provide a "zeroth-order" assessment about which XQQ instruments may have dynamically correct designs, one should determine for each instrument whether or not the σ derived from Equation (1) equals the σ from Equations (2) for a symmetric charge transfer reaction ($\alpha=1$). This provides a very important test that the instrument parameters and the reaction kinetics are well controlled, without having to worry about reaction-induced "mass discrimination" (discussed in Section VI). For collision energies of 1-200 eV, charge transfer reactions are dynamically equivalent to a "worst-case" CAD reaction system because they take place at large impact parameters with near-zero momentum transfer (References 13-16). Thus, the product ions are formed essentially at rest (thermal energies) within Q2.

SECTION III

KEY MS/MS PARAMETERS

There are several parameters (References 5-11) which for any one projectile ion A^+ can cause the relative intensities among its various progeny ions to differ significantly. It is the complex interplay among kinetic and instrument parameters that engenders the necessity for dynamically correct XQQ instruments.

The following are the key parameters which must be controlled if one is to develop and use a generic, instrument-independent MS/MS database.

1. The type of target gas B used (References 17-22); this defines the reaction system $A^+ + B$.
2. The center-of-mass interaction energy E_{cm} for the $A^+ + B$ reaction; the cross section σ and the branching ratios α - δ , etc. depend on E_{cm} . See also Section IV.
3. The target thickness $[B]L$ (References 8-10, 12, 17-20) (refer to constraint 1. of Section II). See also items (6) and (7) below.
4. The difference between the ion source potential and the Q2 rod offset (pole bias) corresponds to the nominal LAB collision energy E_{LAB} (References 8-10).
5. The difference between the ion source potential and the Q1 rod offset influences the resolution within Q1 and determines the nominal energy distribution of the projectile ion beam entering Q2.
6. The Q2 field radius r_0 (in cm) and the Q2 rf frequency F (in MHz) together with the mass m_{react} (in amu) and the axial energy E_{LAB} (in eV) of the reactant (projectile) ion entering Q2; these influence the effective pathlength L_{eff}

of the complex oscillatory trajectory traversed by a projectile ion through Q2. If the actual rectilinear pathlength of the collision region is L_{actual} , then $L_{\text{eff}} = R L_{\text{actual}}$. The correction factor is of the form $R = (1 + (\kappa^2 r_0^2 F^2 m_{\text{react}} / E_{\text{LAB}}))^{0.5}$ and the value for κ depends on the choice of the Mathieu parameter q_2 (rf voltage of Q2) (Reference 8). Note that R depends on $m_{\text{react}} / E_{\text{LAB}}$. Hence, for a given collision energy E_{LAB} the effective target thickness $L_{\text{eff}}[B]$ will be different for different "parents" selected by Q1 for CAD within Q2, and must be corrected accordingly.

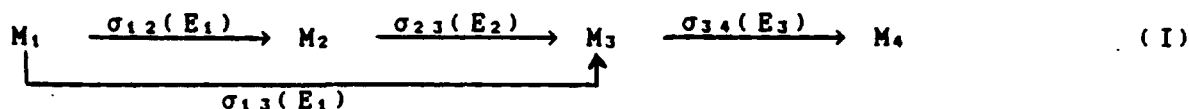
7. The value of q_2 (References 8, 9) and restrictive interquadrupole apertures of diameter $< 1.4 r_0$ (References 8, 23, 24); these determine how effectively parent/daughter ions can be contained within Q2 for emittance (transmission) into Q3 because of mass-dependent focusing effects (refer to constraint 3. of Section II). Strong rf focusing effects within Q2 (maxima and minima in ion transmission as a function of q_2) are especially notable for restrictive interquadrupole apertures when the projectile ion beam has a small energy spread (Reference 8). This will influence the ion trajectory and, therefore, $L_{\text{eff}}[B]$. See Section V for further discussion of q_2 .
8. The difference between the Q2 rod offset and Q3 rod offset determines whether or not some progeny fragment ions can enter Q3 because of the translational energy distribution of the progeny ions (References 9-11, 17-19, 21, 22) (refer to constraint 4. of Section II).
9. The type of detector used [Daly detector, Channeltron (with or without conversion dynode), etc.] because of differences in mass-dependent conversion gain (refer to constraint 2. of Section II).

10. The internal energy of the projectile ion. Dawson's round robin (Reference 12) indicated that the role of excited states could be significant in comparing MS/MS spectra from different laboratories. The type of ionization used (e.g., electron ionization vs. atmospheric-pressure chemical ionization) may influence which of several isomeric structures exit from an ion source (References 25-27). An MS/MS spectrum can depend, therefore, on the type of ionization used (References 25, 27, 28). This was the case for the CAD of benzene, which is strongly dependent on the internal energy of the $C_6H_6^+$ projectile (Reference 28). By contrast, the ratio of $C_7H_7^+/C_7H_8^+$ from the CAD of n-butylbenzene ($C_{10}H_{14}^+$) was found to be independent of the ionizing electron energy over the range 5-25 eV (Reference 29), even though this ratio is known to depend strongly on the internal energy of $C_{10}H_{14}^+$ (Reference 30). Hence, the precollision internal excitation of $C_{10}H_{14}^+$ apparently was lost in transit ($\sim 100 \mu s$) between the ion source and Q2 by some undetermined mechanism (Reference 29).

Parameters 1.-3. are kinetics parameters. Parameters 4.-9. are instrument parameters. Parameter 10. is not discussed further because it is distinct from the focus of this report.

SECTION IV
ENERGY DEPENDENCE OF CAD SPECTRA

Consider the CAD of a "parent" ion M_1^+ selected with Q1.



In this scheme each σ_{ij} represents the absolute cross section of a single elementary reaction; viz., the CAD of an ion M_i^+ to produce directly a "progeny" fragment ion M_j^+ . For a given target gas, each σ_{ij} depends on the effective collision energy E_i for its respective M_i^+ ion [we use $\sigma_{ij}(E_i)$ to represent the functional form of this energy dependence]. For the M_1^+ parent ion, $E_1 = E_{cm}$.

Note that the M_1^+ , σ_{12} , and σ_{13} of scheme (I) correspond, respectively, to the A^+ , $\alpha\sigma$, and $\beta\sigma$ of the kinetic relations (1)-(4) pertinent to single-collision conditions. There is no analogous correspondence for σ_{23} and σ_{34} since these involve multiple-collision conditions.

As discussed below, when multiple-collision conditions are used, secondary collisions of each progeny fragment ion occur with $E_i \neq E_{cm}$ ($i > 1$). Therefore, the choice of single-collision conditions or multiple-collision conditions will determine how E_{cm} influences the observed CAD spectrum (References 9-12, 17-22).

A. SINGLE COLLISIONS:

Variation of E_{cm} under single-collision conditions will cause a change in the relative intensities observed for M_2^+ and

M_3^+ . This change is determined solely by the energy-dependence $\sigma_{12}(E_1)$ for M_2^+ and $\sigma_{13}(E_1)$ for M_3^+ . Here $E_1 = E_{cm}$. Therefore, under single-collision conditions Equations (1)-(4) can provide direct measurements of dynamically correct CAD spectra.

B. MULTIPLE COLLISIONS:

Variation of E_{cm} under multiple-collision conditions will also cause a change in the relative intensities observed for M_2^+ and M_3^+ . But this change is determined by the energy dependences $\sigma_{12}(E_1)$ and $\sigma_{23}(E_2)$ for M_2^+ , and $\sigma_{13}(E_1)$, $\sigma_{23}(E_2)$, and $\sigma_{34}(E_3)$ for M_3^+ . Here again $E_1 = E_{cm}$. But E_2 and E_3 are not equal to E_{cm} .

The relationship between the kinetic energies E_d of daughter ions and E_{cm} is determined by the chemical dynamics of daughter production for each $A^+ + B$ reaction system (References 10, 11, 17-19, 21, 22). Therefore, for the M_1^+ parent ion selected with Q1, its daughters M_2^+ and M_3^+ would undergo secondary collisions with the target gas within Q2 with effective collision energies different from E_{cm} . For the extreme case where M_2^+ and M_3^+ are produced with $E_d = 0$, values for σ_{23} and σ_{34} would correspond to those for thermal collision energies.

Therefore, for progeny ions formed by multiple collisions there is a complex dependence of the cross sections $\sigma_{ij}(E_i)$ on E_{cm} (References 10, 11, 17-19, 21, 22). To measure dynamically correct CAD spectra under multiple-collision conditions, corrections would have to be made for the variable energy-dependence of the cross sections of all daughters for each E_{cm} ; for multiple-collision-induced scattering losses (References 23, 24); etc. Such corrections are not feasible in XQQ instruments because of the complex interplay among the key MS/MS parameters (Section III).

C. E_{cm} :

To facilitate the discussion above, we have used E_{cm} to designate the center-of-mass interaction energy. It is important to note, however, that the center-of-mass interaction energy available for internal excitation to produce CAD depends on the molecular dynamics of the $A^+ + B$ interaction. There are two dynamical extremes possible (References 31-35). In the "elastic" limit, polyatomic species A^+ and B would interact as rigid entities and $E_{cm} = \frac{1}{2}\mu v^2 =$ kinetic energy of relative motion ($\mu = m_A m_B / (m_A + m_B)$ and $v =$ velocity of A^+ relative to B). In the "spectator" or "binary" limit, only the "impact" moieties of polyatomic species A^+ and B would interact with each other; the "nonimpact" moieties are merely "spectators" (i.e., they are unaffected by the interaction between the "impact" moieties). Because of a lack of knowledge about the details of the CAD dynamics, the work cited above (References 10, 11, 17-19, 21, 22) defines E_{cm} in the context of the "elastic" limit. The "elastic" limit provides a dynamically correct representation for the low-energy CAD of CH_4^+ with a helium target (References 34, 35).

SECTION V REACTION-INDUCED MASS DISCRIMINATION

The value of the Mathieu parameter q for any ion of mass m determines how well that ion is contained within a quadrupole mass filter (References 5, 6, 8). For a given q , ions of different masses will have different transmission efficiencies. Any ion will follow an unstable trajectory when its q exceeds 0.908 (the stable-trajectory limit) (Reference 8).

When reaction occurs within Q2 there is a sudden change in mass from the reactant ion mass, m_{react} , to a product ion mass, m_{prod} . Therefore, there is a reaction-induced "mass discrimination" within Q2 due to $q_{\text{prod}} = q_{\text{react}} \cdot m_{\text{react}}/m_{\text{prod}}$ (References 5, 6, 8). That is, the reactant ion and each of its product ions all have different ion containment efficiencies. Here q_{prod} and q_{react} are, respectively, the Mathieu parameters of the product ($_{\text{prod}}$) and reactant ($_{\text{react}}$) ions within Q2.

One can have $m_{\text{prod}} > m_{\text{react}}$ if the reaction involves adduct formation within Q2 ("neutral gain" experiments), or conceivably also if there is reaction-induced fragmentation (RIF) subsequent to adduct formation (References 1-3). In these cases the Mathieu parameter q_{prod} for product ions would always be smaller than the q_{react} for reactant ions. Therefore, when $m_{\text{prod}} > m_{\text{react}}$, the product ions always follow stable trajectories within the Q2Q3 structure (so long as $q_{\text{react}} < 0.908$). This situation contrasts significantly from CAD.

For CAD, $m_{\text{prod}} < m_{\text{react}}$ and $q_{\text{prod}} > q_{\text{react}}$ within Q2. Therefore, low-mass daughters can never be detected within XQQ instruments when $m_{\text{prod}} < m_{\text{react}} \cdot q_{\text{react}}/0.908$ within Q2. Note, however, that Equations (2)-(4) would allow one to estimate what fraction of the product ions are missing ($=1-(\alpha+\beta+\dots)$).

This analysis suggests that a demand for dynamically correct performance within XQQ instruments favors the use of RIF (or adduct formation), if possible, instead of CAD.

SECTION VI GENERIC MS/MS DATABASE

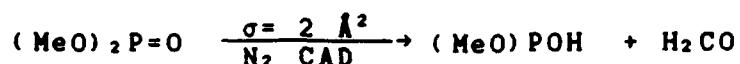
The discussion in this Section refers to Reaction Scheme (I) (Section IV) in the context of Equations (2)-(4).

To be generic, a MS/MS database must be a dynamically correct (instrument-independent) representation of the $\sigma_{ij}(E_i)$ (viz., the $\alpha\sigma$, $\beta\sigma$, etc. of Equations (2)-(4)). That is, the ion signals measured for C^+ , D^+ , etc. must correspond to those represented by Equations (2)-(4). Therefore, the ion signal corresponding to each σ_{ij} must be measured under well-defined (E_i , [B], etc.) single-collision conditions. For example, for a given target gas B, the ion signal corresponding to $\sigma_{34}(E_3)$ would have to be measured as a function of E_3 and of [B] by selecting M_3^+ as the "parent" ion.

For a QQQ instrument this presumes that Q1 can be used to select each of the progeny ions M_i^+ ($i > 1$) as the "parent" ion before the entry of the M_i^+ ion ($i > 1$) into Q2. This requires that each M_i^+ ion ($i > 1$) must be produced with good intensity before its entry into Q1. This may not always be easy in a QQQ instrument.

In the case of a Q1Q2Q3Q4Q5 multiquadrupole instrument, Q2 and Q4 could be used as reactive collision regions, while Q1, Q3, and Q5 would be analyzing mass filters. Q2 would be operated under multiple-collision conditions to provide an intense source of M_i^+ ions ($i > 1$). Q4 would be operated under single-collision conditions. Then the σ_{ij} ($i > 1$, $j > 1$) could be measured by using gas in both Q2 and Q4. The σ_{1j} ($j > 1$) would be measured by using gas in Q4, but no gas in Q2.

Dawson and coworkers (Reference 10) demonstrated that it is plausible to associate a $\sigma_{ij}(E_i)$ with the CAD of a specific ionic substructure. For example (see Reference 10),



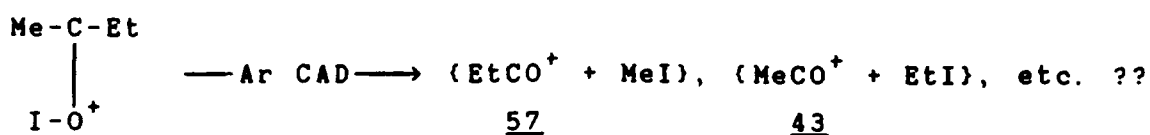
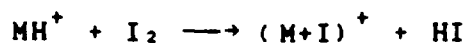
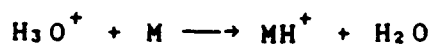
Therefore, one can envision a generic CAD database comprised of critically-evaluated $\sigma_{ij}(E_i)$ and product identities [e.g., $(\text{MeO})\text{POH}^+$] for CAD of known ionic substructures [e.g., $(\text{MeO})_2\text{P}=\text{O}^+$]. The advantages of such a database are:

1. The cross sections would characterize the CAD spectra of both known and unknown species (so long as the unknown species contain ionic substructures for which the CAD cross sections and product identities are known): <Consider a simplistic analogy where compounds correspond to words, and substructures correspond to letters: thousands of words can be composed with only 26 letters of the alphabet>;
2. Characterization of an unknown is not limited by the number of compounds in a "library";
3. The format is compatible with its use in expert systems;
4. End users are involved directly in its evolution by using critically evaluated cross sections already in the database and by submitting new cross sections for inclusion in the database.

The problem with CAD, however, is that it is not species-specific. If two molecules form the same "parent" ion structure, then the CAD fragmentations will be identical, and the two species are indistinguishable. That is, the σ_{ij} are not unique for the CAD of polyatomic isomers. For example, 2-butanone $(\text{MeC}(=\text{O})\text{Et})$ and 2,3-epoxybutane $(\text{MeC}(\text{H})-\text{C}(\text{H})\text{Me}-\text{O})$ give substantially identical CAD spectra (Reference 36).

However, it may be possible to distinguish among isomeric compounds by using species-specific ion chemistry within an ion

source in conjunction with CAD within Q2. For example, to distinguish M= 2-butanone from M= cis-2,3-epoxybutane (both m/z 72), one can react I₂ with the protonated molecule MH⁺ to prepare an (M+I)⁺ product ion (m/z 199). The CAD (Ar target) of the (M+I)⁺ ion gives a m/z 44 fragment for cis-2,3-epoxybutane but not for 2-butanone (Reference 36). The mechanism was not established, but may correspond to the following.



The database concepts in this Section can be applied equally well to reactions other than CAD. Based on the dynamics given in Section V, reactions of $m_{\text{prod}} > m_{\text{react}}$ are to be preferred over CAD. Therefore, one can envision the use of reactions other than CAD whose $\sigma_{ij}(E_i)$ and product identities would uniquely characterize a specific ionic substructure.

A trivial example of this concept is the reaction $\text{N}_2^+ + \text{SF}_x \rightarrow \text{N}_2 + \text{SF}_x^+$ (x=1-5), where SF_x would be considered a "species-specific" reactant for N₂⁺ in the sense that the $\sigma_{ij}(E_i)$ ($\alpha\sigma$, $\beta\sigma$, etc. of Equations (2)-(4)) would be unique to N₂⁺. Thus, one could distinguish N₂⁺ from CO⁺ or C₂H₄⁺ because the analogous reactions of SF_x with CO⁺ or C₂H₄⁺ are endoergic by 0.45 eV and 3.96 eV, respectively (i.e., no SF_x⁺ would be produced as $E_{\text{cm}} \rightarrow 0$). Or, for example, one can distinguish among isomeric C₃H₃⁺ structures on the basis of differences in their

reactivities with "specific" reactants (i.e., different $\sigma_{ij}(E_i)$ for different isomers). The ability to discriminate among structures on the basis of chemical reactivity has been demonstrated under thermal reaction conditions (References 37-41). Note, however, that this approach can only be used when there are large differences in reactivity between isomeric ions. This may not always be the case. The RIF reactions of References 1-3 provide other examples.

Constraint 3. of Section II provides another important reason why adduct formation is to be preferred over CAD. To achieve 100 Percent collection efficiency for progeny ions, one must use a withdrawing potential to extract the ions from Q2 into Q3 (i.e., the Q3 rod offset must be biased negatively with respect to the Q2 rod offset) (References 1-3, 42-45). Under such conditions one observes a poorly resolved MS/MS spectrum in Q3 (Reference 11). Hence, it would not be possible to make a dynamically correct determination of the relative abundance of progeny ions which are separated by only a few amu. For example, under such low-resolution conditions it would not be possible to distinguish $C_7H_7^+$ (m/z 91) from $C_7H_8^+$ (m/z 92) when formed by the CAD of n-butylbenzene. In contrast, even under low-resolution conditions adduct formation can provide a unique species-specific product which can be well separated in mass from the parent ion. For example, under typical MS/MS operating conditions, the reaction of an acyl ion (RCO^+) of mass M with 2-butanone (mass 72) forms an adduct of mass (M+72) which can be used to characterize the RCO^+ ionic substructure (e.g., $MeCO^+ + MeC(=O)Et \rightarrow$ adduct at m/z 115; $EtCO^+ + MeC(=O)Et \rightarrow$ adduct at m/z 129) (Reference 46).

SECTION VII EXPERIMENTAL VALIDATION

This Section describes the experimental protocol, shows typical $\ln Y$ and $\ln W$ plots, and discusses how the experimental data conform to the kinetic Equations (1)-(4).

The experimental protocol is presented in the context of how the measurements were made for the study of the reaction $N_2^+ + SF_6 \rightarrow N_2 + SF_x^+$ ($x=1-5$) (Reference 42). We used $N_2^+ + SF_6 \rightarrow N_2 + SF_x^+$ ($x=1-5$) to evaluate which corrections are necessitated by reaction-induced "mass discrimination" [the mass m_{prod} of each of the SF_x^+ products is larger than the mass m_{react} of the N_2^+ reactant (Reference 42)]. Analogous measurements were made for the study of the reactions $Ne^+ + Ne \rightarrow Ne + Ne^+$ (Reference 43), $Ar^+ + Ar \rightarrow Ar + Ar^+$ (Reference 44), and $Ar^+ + N_2 \rightarrow Ar + N_2^+$ (Reference 45). These reactions were studied to kinetically validate the effective gas target thickness.

Note that $Ne^+ + Ne \rightarrow Ne + Ne^+$, $Ar^+ + Ar \rightarrow Ar + Ar^+$, and $Ar^+ + N_2 \rightarrow Ar + N_2^+$ are charge transfer reactions, while $N_2^+ + SF_6 \rightarrow N_2 + SF_x^+$ ($x=1-5$) is a dissociative charge transfer reaction. For collision energies of 1-200 eV, charge transfer reactions are dynamically equivalent to a "worst-case" CAD reaction system because they take place at large impact parameters with near-zero momentum transfer (References 13-16). Thus, the product ions are formed essentially at rest (thermal energies) within Q2.

Work from this laboratory (References 42-45) has demonstrated that dynamically correct branching ratios α , β , ..., etc. can be measured in our QQQ instrument (Reference 47) when the key MS/MS parameters are properly selected.

A. EXPERIMENTAL PROTOCOL

All experiments were carried out in the NBS QQQ instrument (see Figure 1). It has been described in detail elsewhere (Reference 47).

The instrument conforms to the design considerations stipulated by Dawson and coworkers (References 8-10) for close-coupled quadrupoles. The instrument can be configured to use either a molecular beam or collision chamber configuration. The collision chamber configuration was used here.

Briefly, as shown in Figure 1, the instrument consists of (i) a standard electron impact ionizer, (ii) three standard quadrupole rod assemblies (Q1, Q2, Q3) operated in phase at 1.2 MHz and mounted in tandem on a special multipurpose track, and (iii) a continuous-dynode electron multiplier which incorporates a conversion dynode. Q2 is surrounded by a collision chamber enclosure while Q1 and Q3 have no housing, and are adequately pumped by four 1200 L/s turbomolecular pumps, ensuring a well-defined collision region.

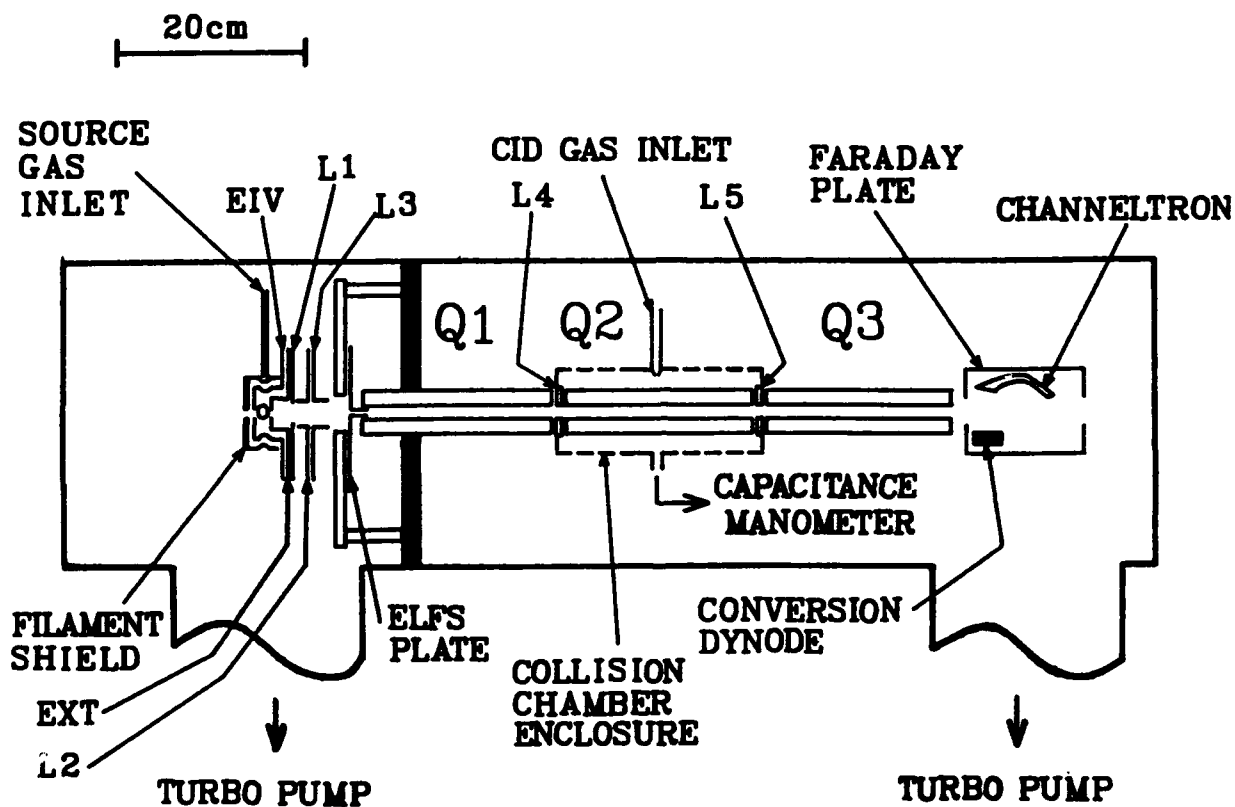


Figure 1. Schematic of NBS QQQ Instrument. EIV, EXT, L1-L5, etc., are Ion Optical Lens Elements.

The actual rectilinear pathlength of the collision region is $L_{\text{actual}} = 21.745 \pm 0.075$ cm. However, the effective target thickness for a projectile ion A^+ in target gas B is $L_{\text{eff}}[B]$. Here $L_{\text{eff}} = R L_{\text{actual}}$ is the effective pathlength of the complex oscillatory trajectory traversed by a projectile ion through the target gas when Q2 is operated with $q_2 = 0.28$ (Reference 8). The subscript (2) of q_2 is used to designate the Mathieu parameter q for Q2. The R correction factor is given (Reference 8) by

$$R = [1 + (0.0738 r_o^2 F^2 M/E)]^{0.5} \quad (5)$$

and is approximately 1.01 at $E = 60$ eV and 1.13 at $E = 5$ eV for our instrument ($r_o =$ field radius = 0.684 cm (quadrupole rod diameter = 1.59 cm), $F =$ rf frequency = 1.2 MHz; $M =$ mass of projectile ion (in amu), $E =$ axial ion energy (in eV)).

Reaction cross sections σ were derived by using Equations (1)-(4). In this report, A^+ , B, α , β , γ , δ , and ϵ correspond, respectively, to N_2^+ , SF_6 , SF_5^+ , SF_4^+ , SF_3^+ , SF_2^+ , and SF^+ . For each interaction energy E, we shall use $\sigma_{\text{Ln } \gamma}$ and $\sigma_{\text{Ln } W}$ to designate the σ values derived from Ln Y measurements and from Ln W measurements, respectively. All kinetic measurements were based on operation of Q2 with its Mathieu parameter q_2 (References 5, 6) set to the individual values of q which corresponded to the maximum ion transmission through Q2Q3 for N_2^+ ($\langle q_{\text{react}} \rangle_{\text{max}}$) or for each of the SF_x^+ ($x=1-5$) products ($\langle q_{\text{prod}} \rangle_{\text{max}}$).

Note that the extent of reaction is determined by $\sigma(B)L$ (Equations (1)-(4)). For a particular $A^+ + B$ interaction at a given collision energy E_{coll} , $\sigma(B)$ is constant for a given [B]. However, the pathlength L is influenced by the choice of q_2 (Reference 8). Therefore, since q_2 is changed for each ion detected, the extent of reaction which is observed for the decay of N_2^+ and for the production of each of the SF_x^+ corresponds to different effective pathlengths for each ion. We use L_{A^+} , L_α , L_β , etc. to designate, respectively, the effective pathlengths

for N_2^+ , SF_5^+ , SF_4^+ , etc. Consequently, α , β , etc. are estimated from $\ln W_\alpha = \sigma(B)L_\alpha$, $\ln W_\beta = \sigma(B)L_\beta$, etc. by using the σ derived from $\ln Y = \sigma(B)L_{A^+}$ (i.e., if $\alpha + \beta + \dots = 1$, then $\sigma_{\ln W} = \sigma_{\ln Y}$).

The L_{A^+} , L_α , L_β , etc. (at their respective q_2 values) were determined relative to L_{eff} (calculated from Equation (5) for $q_2 = 0.28$) by measuring $\ln Y$ vs. q_2 for $q_2 \approx 0.1-0.7$ at an arbitrary, constant $[B]$ for each E_{coll} used in the experiments. Under these conditions, $\sigma(B) = \text{constant}$, so that

$$R_{A^+} \equiv L_{A^+}/L_{eff} \\ = \{(\ln Y \text{ at } q_2 = \langle q_{react} \rangle^{max}) / (\ln Y \text{ at } q_2 = 0.28)\}$$

$$R_\alpha \equiv L_\alpha/L_{eff} \\ = \{(\ln Y \text{ at } q_2 = \langle q_{prod} \rangle^{max} \text{ for } SF_5^+) / (\ln Y \text{ at } q_2 = 0.28)\}$$

$$R_\beta \equiv L_\beta/L_{eff} \\ = \{(\ln Y \text{ at } q_2 = \langle q_{prod} \rangle^{max} \text{ for } SF_4^+) / (\ln Y \text{ at } q_2 = 0.28)\},$$

etc.

Appropriate corrections were also made for (i) the detector's conversion gain for each product ion relative to that for N_2^+ (approximately 0.9 for SF_5^+); (ii) for contributions from X S isotopes ($[^X SF_5^+] \approx 1.05 [^{32} SF_5^+]$ for $X=32+33+34+36$); and (iii) for differences in ion transmission efficiencies between N_2^+ and each of the SF_x^+ ($x=1-5$) (in the next paragraph we describe the method used to estimate these relative transmission corrections).

If one were to select a value of q_2 which corresponds to $\langle q_{react} \rangle > 0.908$ but to $\langle q_{prod} \rangle < 0.908$, then the N_2^+ reactant ion would not be transmitted through Q2, but an SF_x^+ product ion would be transmitted. If SF_x^+ product ions were to be observed when $\langle q_{react} \rangle > 0.908$, then these SF_x^+ ions would have to be formed by $N_2^+ + SF_6$ interactions occurring outside Q2. Thus, the experimentally-measured SF_x^+ ion signal (represented by $[SF_x^+]_{exp}$) can consist of SF_x^+ ions produced within Q2

(represented by $[SF_x^+]_{Q2}$) and outside Q2 (represented by $[SF_x^+]_{notQ2}$). That is, $[SF_x^+]_{exp} = [SF_x^+]_{Q2} + [SF_x^+]_{notQ2}$. However, in Equations (2), (3) one must use the $[SF_x^+]_{Q2}$ measured at $\langle q_{prod} \rangle^{max}$. Since $[SF_x^+]_{Q2} = [SF_x^+]_{exp} - [SF_x^+]_{notQ2}$, one must estimate $[SF_x^+]_{notQ2}$. This was done by measuring $[SF_x^+]_{exp}$ vs. q_{prod} for each SF_x^+ ion for $q_{prod} \approx 0.1-0.7$ at an arbitrary,

constant $[SF_6]$ for each E_{coll} used in these experiments. For $q_{react} > 0.908$, the $[SF_x^+]_{exp}$ vs. q_{prod} plots are nearly linear, and were back-extrapolated to the q_{prod} corresponding to $q_{react} = 0.908$ (where the N_2^+ trajectories become unstable). We equated $[SF_x^+]_{notQ2}$ with the value of $[SF_x^+]_{notQ2}$ obtained by this linear back-extrapolation. Hence, our estimate of $[SF_x^+]_{Q2}$ at $\langle q_{prod} \rangle^{max}$ corresponds to $\langle 1 \rangle$ minus $\langle 2 \rangle$, where

$\langle 1 \rangle =$ (the value of $[SF_x^+]_{exp}$ measured at $\langle q_{prod} \rangle^{max}$),

$\langle 2 \rangle =$ (the value of $[SF_x^+]_{notQ2}$ at the back-extrapolated $q_{react} = 0.908$),

and

$\langle RTC \rangle \equiv$ Relative Transmission Correction = $(1 + (\langle 2 \rangle / \langle 1 \rangle))$.

Hence, $[SF_x^+]_{Q2} = [SF_x^+]_{exp} / \langle RTC \rangle$. $\langle RTC \rangle$ values range from 1.0-1.2 for each product ion (Reference 42).

High-purity SF_6 (>99.99 Percent) was used as the target gas without further purification. Single-collision conditions correspond to $L[SF_6] \leq 2.25$ cm-mtorr. Pressure measurements in the center of the collision chamber were made with a 1 torr capacitance manometer (appropriate corrections were made for thermal transpiration (≈ 3 Percent), etc.). To minimize the possibility of incurring systematic errors in the measured cross sections due to errors in the pressure measurements, our measurements of $\ln Y$ and $\ln W$ [Equations (1)-(4)] are made at several target gas pressures rather than at a single pressure (refer to Figure 1(a)).

N_2^+ ions were generated by 70 eV electron impact, and the N_2^+ projectiles were selected by Q1. The energy spread of the projectiles entering Q2 was determined to be ≤ 1.6 eV for 50

Percent of the ions, ≤ 2.7 eV for 90 Percent of the ions, and ≤ 4.1 eV for 99 Percent of the ions when measured by using the Q2 pole bias (rod offset) to generate a stopping potential curve. E_{50} , E_{90} , and E_{99} correspond, respectively, to the Q2 potential required to stop 50 Percent, 90 Percent, and 99 Percent of the projectile ions entering Q2. The collision energy E_{coll} was selected by setting the Q2 pole bias = $E_{50} - E_{coll}$. (For a given Q2 pole bias, if E_{coll} were to be defined by using E_{90} instead of E_{50} , then the center-of-mass interaction energy E_{cm} corresponding to E_{coll} would be only 0.9 eV higher with E_{90} than with E_{50} .)

The N_2^+ projectiles entering Q2 are substantially pure ground-state $X \ ^2\Sigma_g^+$. This is supported by the following facts. In addition to the $X \ ^2\Sigma_g^+$ ground state of N_2^+ , $A \ ^2\Pi_u$ and $B \ ^2\Sigma_u^+$ are the only excited states of N_2^+ which are produced in significant concentrations by electron ionization. The lifetimes of these excited states are $< 17 \mu s$ and $< 0.07 \mu s$, respectively. However, the ion transit time through Q1 is approximately 45 μs . Therefore, the A and B states are substantially quenched before N_2^+ enters Q2. This was validated experimentally. For $E_{coll} = 40$ eV we found $\sigma_{Ln Y}$ was independent of the ionizing electron energy E_e for $E_e = 16-70$ eV.

Measurements of reactant ion loss and product ion formation ($\ln Y$ and $\ln W$ measurements; Equations (1)-(4)) were performed at each selected collision energy by setting the Q3 pole bias sufficiently negative relative to the Q2 pole bias ($Q2-Q3 \approx 90$ to 145 V for $E_{coll} \approx 60$ to 5 eV) to insure that all ions (products and unreacted projectiles) were drawn out of Q2 into Q3. These parameter settings are consistent with the knowledge that for $E_{coll} = 1-200$ eV (LAB) charge transfer reactions take place at large impact parameters with near-zero momentum transfer (References 13-16). The typical ion collection efficiency is ≥ 99 Percent; i. e., the total ion current for products + unreacted projectiles ≥ 99 Percent of the initial projectile ion current.

This high ion collection efficiency allows one to use Equations (2), (3).

B. RESULTS

Plot (a) of Figure 2 shows typical data for projectile ion decay ($\ln Y$ vs. P measurements based on Equation (1)). Plot (b) of Figure 2 shows the energy dependence of the reaction cross section when $\sigma_{\ln Y}$ values are plotted versus their respective center-of-mass interaction energies E_{cm} . The $\sigma_{\ln Y}$ values were derived from measurements of $\ln Y$ vs. $\sigma L[SF_6]$ (Equation (1)), corrected for relative differences in the effective pathlengths L_{A^+} , L_{α} , L_{β} , etc. Plots (a)-(d) of Figure 3 show typical data for product ion growth for $N_2^+ + SF_6 \rightarrow N_2 + SF_x^+$ ($x=2-5$) (measurements of $\ln W_{\alpha}$, etc. vs. P ; based on Equations (2), (3)). Analogous results were obtained for $Ne^+ + Ne \rightarrow Ne + Ne^+$ (Reference 43), $Ar^+ + Ar \rightarrow Ar + Ar^+$ (Reference 44), and $Ar^+ + N_2 \rightarrow Ar + N_2^+$ (Reference 45).

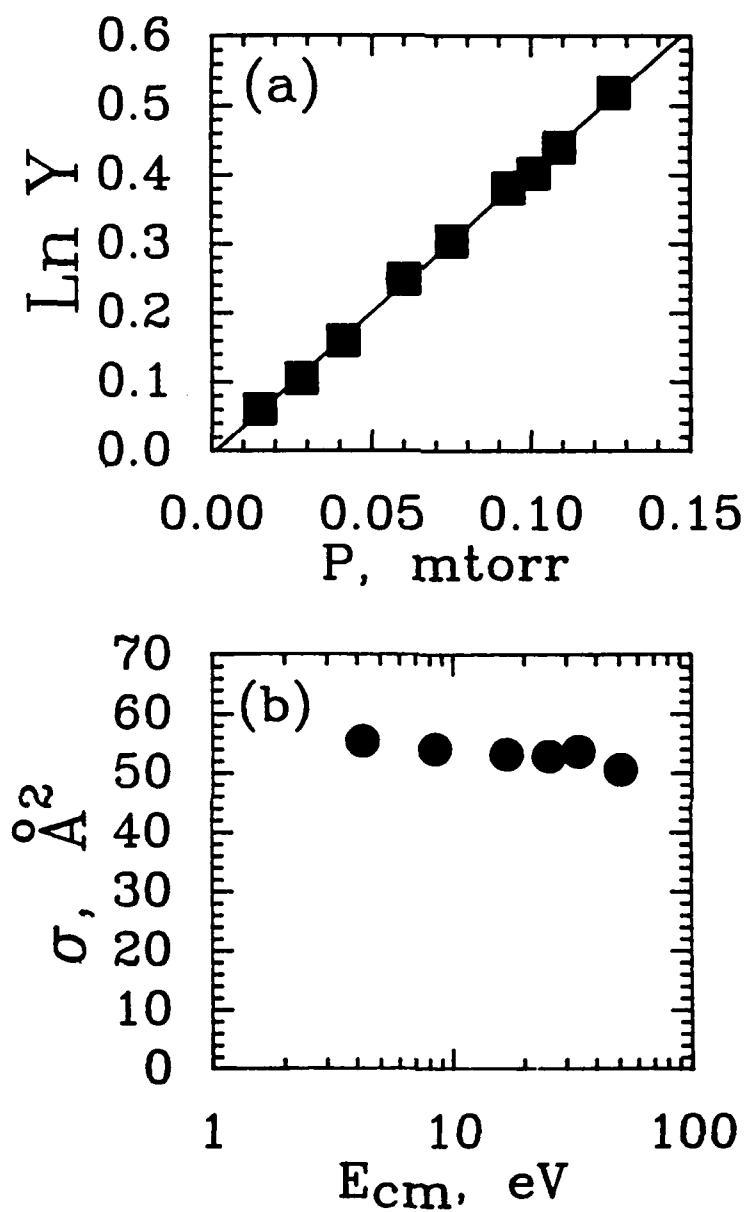


Figure 2. Plots of (a) $\text{Ln } Y$ vs. SF_6 Target Pressure P for $E_{\text{coll}} = 40$ eV (LAB) and (b) of σ vs. E_{cm} .

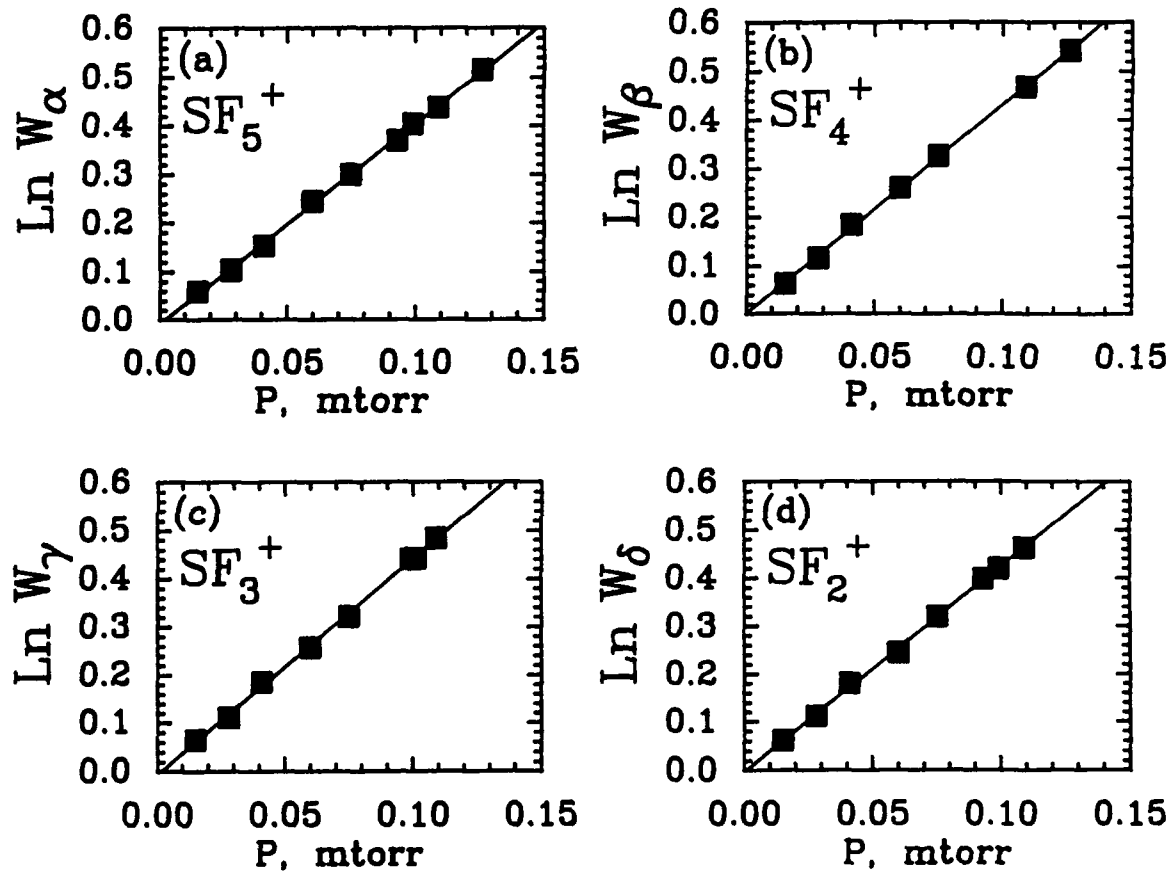


Figure 3. Plots of $\text{Ln } W_i$ ($i=\alpha$ to δ) vs. SF_6 Target Pressure P for $E_{\text{coll}} = 40 \text{ eV (LAB)}$.

C. DISCUSSION

In conformance with the kinetic Equations (1)-(4), excellent linear plots were observed in every case (References 42-45) for $\ln Y$ vs. P and $\ln W$ vs. P under single-collision conditions. Moreover, we found that $\alpha + \beta + \gamma + \delta + \epsilon = 1.0 \pm 0.1$ (i.e., $\sigma_{\ln Y}$ derived from Equation (1) equals $\sigma_{\ln W}$ from Equations (2), (3) (References 42-45)). Therefore, our σ values are substantially free from kinetic interferences (i.e., no back reactions, no impurity reactions, no scattering losses, minimal fringing fields, no mass discrimination, well-defined gas target, etc.).

These studies demonstrate that careful control of the key MS/MS parameters ($\langle q_{\text{react}} \rangle^{\text{max}}$, $\langle q_{\text{prod}} \rangle^{\text{max}}$, etc.) makes it possible to account properly for the reaction-induced mass discrimination which occurs intrinsically within the Q2 of a dynamically correct XQQ instrument. Consequently, by following the protocol of Section VII A., the reaction $N_2^+ + SF_6 \rightarrow N_2 + SF_6^+$ ($x=1-5$) can be used to assess which XQQ instruments have dynamically correct designs.

As discussed in Section I B., the spectrum which is observed for any CAD process is determined by the extent of reaction. The extent of reaction, in turn, is determined by $\sigma(B)L$. Hence, the absolute target thickness $[B]L$ is a critical parameter which must be accurately known if a generic MS/MS database is to be developed.

We have demonstrated that it is possible to kinetically validate the absolute target thickness in a dynamically correct XQQ instrument to within ± 10 Percent (in-situ calibration). Hence, one can determine the absolute target thickness for Ne, Ar, and N_2 gas targets by using Equations (1)-(4) together with the σ values for $Ne^+ + Ne \rightarrow Ne + Ne^+$ (Reference 43), $Ar^+ + Ar \rightarrow Ar + Ar^+$ (Reference 44), and $Ar^+ + N_2 \rightarrow Ar + N_2^+$ (Reference 45), respectively. For these reactions $\alpha=1$.

There is probably no significant systematic error in our measurements of the absolute total cross sections. Our σ values

for $\text{Ne}^+ + \text{Ne} \rightarrow \text{Ne} + \text{Ne}^+$ (Reference 43) and $\text{Ar}^+ + \text{Ar} \rightarrow \text{Ar} + \text{Ar}^+$ (Reference 44) agreed to within ± 10 Percent with experimental and theoretical results from the literature. Therefore, the largest absolute uncertainty in the experimentally-determined effective target thickness $(L)_{\text{eff}}$, and therefore in our σ values, is probably on the order of ± 10 Percent. This ± 10 Percent error estimate is also consistent with our observations that deviations from linearity in $\ln W$ vs. P plots (refer to Equation (2)) occurred only when single-collision conditions were exceeded (i.e., when $(L)_{\text{eff}}/\lambda \geq 1.0-1.1$, where $\lambda =$ mean free path). Hence, single-collision conditions must be used if one is to develop and use a generic, instrument-independent MS/MS database (Reference 44).

Reactant ions and product ions behave differently within the Q1Q2Q3 structure (References 5-11). Therefore, the difference between $\sigma_{\text{Ln } Y}$ and $\sigma_{\text{Ln } W}$ (i.e., how closely the sum $\alpha + \beta + \gamma + \delta + \epsilon$ approximates 1.0) can provide a measure of how well confined a gas target is within Q2. If they differ by z Percent, then the largest relative uncertainty in the effective target thickness $(L(B))$ would be on the order of $2z$ Percent for a target gas which is not substantially confined within Q2. Our study of the reactions $\text{N}_2^+ + \text{SF}_x \rightarrow \text{N}_2 + \text{SF}_x^+$ ($x=1-5$) (Reference 42), $\text{Ne}^+ + \text{Ne} \rightarrow \text{Ne} + \text{Ne}^+$ (Reference 43), $\text{Ar}^+ + \text{Ar} \rightarrow \text{Ar} + \text{Ar}^+$ (Reference 44), and $\text{Ar}^+ + \text{N}_2 \rightarrow \text{Ar} + \text{N}_2^+$ (Reference 45) indicates that for the worst case z Percent ≤ 6 Percent (but more typically < 2 Percent).

SECTION VIII
ROUND ROBIN FOR XQQ INSTRUMENTS

A Round Robin has been organized by the author to provide a "zeroth-order" assessment about which XQQ instruments may have dynamically correct designs, and may be well-suited for the generation of a generic MS/MS database. Several investigators have agreed to participate. A test protocol is being formulated. It will involve:

1. In situ target thickness calibration within the collision region of each participant's XQQ instrument (a calibration curve will be provided by the author so that Equations (1) and (2) can be used with $\text{Ar}^+ + \text{Ar} \rightarrow \text{Ar} + \text{Ar}^+$ (Reference 44) to determine the target thickness [BIL], followed by
2. Use of Equations (1) and (2) with $\text{N}_2^+ + \text{SF}_6 \rightarrow \text{N}_2 + \text{SF}_5^+$ to assess how well one can correct for reaction-induced "mass discrimination" in various XQQ instruments.

As a precursor to this Round Robin, we organized a Workshop to try to reach a consensus among participants as to the needs of the analytical community for a MS/MS CAD database (see Workshop Report in APPENDIX A).

SECTION IX CONCLUSIONS AND RECOMMENDATIONS

A. CONCLUSIONS

As detailed in Sections III-V, the kinetic parameters and instrument parameters are interrelated in a complex way. For example, the effective target thickness (a kinetic parameter) depends on the r_0 and F of Q2, etc. (Section III). Therefore, it is not possible in practice to standardize XQQ instruments on the basis of the kinetic parameters alone. This was demonstrated by Dawson's round robin (Reference 12).

Single-collision conditions must be used if one is to develop and use a generic, instrument-independent MS/MS database (Reference 44). Under multiple-collision conditions different XQQ instrument designs will suffer differences in ion containment efficiencies depending on whether or not they have restrictive interquadrupole apertures (References 8, 23, 24), close-coupled design (References 8-10), etc. That is, the complex ion-optical effects will produce different degrees of reactive and nonreactive scattering losses within different Q2Q3 structures [refer to References 23 and 24]. Corrections are not feasible (Section IV).

Consequently, multiple-collision conditions can generate instrument-dependent, dynamically distorted CAD spectra because of the complex interplay among the key MS/MS parameters. MS/MS analytical techniques which employ multiple-collision conditions to maximize daughter ion production cannot, in principle, generate instrument-independent MS/MS CAD spectra. The very high CAD efficiency (approximately 100 Percent) observed for MS/MS in quadrupole ion traps (Reference 48) indicates that multiple-collision conditions predominate under typical operating conditions [ion trapping times of 1-100 ms and approximately 1 mtorr (0.133 Pa) of He buffer gas (References 48, 49)].

For the dynamical reasons presented throughout this report, XQQ instruments intrinsically favor the use of reactions wherein $m_{\text{prod}} > m_{\text{react}}$. Adduct formation (or RIF) can potentially satisfy this condition. However, adduct formation requires multiple-collision conditions, and therefore is dynamically not suitable for the development of a generic, quantitatively correct MS/MS database.

Further work is needed to assess which ion-molecule reactions can uniquely characterize ionic substructures by functional class under dynamically correct conditions. Note, however, that for structural characterization of an unknown (qualitative analysis) one can use presence/absence algorithms such as those discussed by Enke and coworkers (Reference 50).

For polyatomic ions, strong increases in the branching ratios α - δ as a function of increasing E_{cm} may be due (a) to the opening of endoergic channels or (b) to the choice of key MS/MS parameters which do not provide dynamically correct operating conditions.

B. RECOMMENDATIONS

We must obtain a "zeroth-order" assessment of which XQQ instruments have dynamically correct designs before the analytical community can decide which type of generic, instrument-independent MS/MS database ought to be developed (refer to Section VIII).

REFERENCES

1. Schmit, J. P., Dawson, P. H., and Beaulieu, N., "Chemical Synthesis Inside the Collision Cell of a MS-MS System. 1. Formation of Adduct Ions Between Protonated Esters and Ammonia," Organic Mass Spectrometry, Vol. 20, pp. 269-275, 1985.
2. Schmit, J. P., Beaudet, S., and Brisson, A., "Ion Molecule Reaction Inside the Collision Cell of a Tandem Quadrupole Mass-Spectrometric System. 2. Energy-Dependence of Ammonium Ion Formation," Organic Mass Spectrometry, Vol. 21, pp. 493-498, 1986.
3. Schmit, J. P. and Beaudet, S., "Formation of Adduct Ions by Ion-Molecule Reaction in Multiple-Stage Ultralow-Axial-Kinetic-Energy Mass Spectrometry," Spectroscopy (Ottawa), Vol. 4, pp. 137-51, 1985.
4. Yost, R. A. and Fetterolf, D. D., "Tandem Mass-Spectrometry (MS/MS) Instrumentation," Mass Spectrometry Reviews, Vol. 2, pp. 1-45, 1983.
5. Dawson, P. H., Quadrupole Mass Spectrometry and Its Applications, Elsevier, Amsterdam, 1976.
6. Dawson, P. H., "Ion Optical-Properties of Quadrupole Mass Filters," Advances in Electronics and Electron Physics, Vol. 53, pp. 153-208, 1980.
7. Dawson, P. H., "Energetics of Ions in Quadrupole Fields," International Journal of Mass Spectrometry and Ion Processes, Vol. 20, pp. 237-245, 1976.
8. Dawson, P. H. and Fulford, J. E., "The Effective Containment of Parent Ions and Daughter Ions in Triple Quadrupoles Used for Collisional Dissociation," International Journal of Mass Spectrometry and Ion Processes, Vol. 42, pp. 195-211, 1982.
9. Dawson, P. H., French, J. B., Buckley, J. A., Douglas, D. J., and Simmons, D., "The Use of Triple Quadrupoles for Sequential Mass-Spectrometry .1. The Instrument Parameters," Organic Mass Spectrometry, Vol. 17, pp. 205-211, 1982.
10. Dawson, P. H., French, J. B., Buckley, J. A., Douglas, D. J., and Simmons, D., "The Use of Triple Quadrupoles for Sequential Mass-Spectrometry .2. A Detailed Case-Study," Organic Mass Spectrometry, Vol. 17, pp. 212-219, 1982.

11. Shushan, B., Douglas, D. J., Davidson, W. R., and Nacson, S., "The Role of Kinetic-Energy in Triple Quadrupole Collision-Induced Dissociation (CID) Experiments," International Journal of Mass Spectrometry and Ion Processes, Vol. 46, pp. 71-74, 1983.
12. Dawson, P. H. and Sun, W. F., "A Round Robin on the Reproducibility of Standard Operating-Conditions for the Acquisition of Library MS/MS Spectra Using Triple Quadrupoles," International Journal of Mass Spectrometry and Ion Processes, Vol. 55, pp. 155-170, 1984.
13. Kaiser, E. W., "Crossed-Molecular-Beam Study of Kinematics and Dynamics of Charge-Transfer Collisions," Journal of Chemical Physics, Vol. 61, pp. 2720-2726, 1974.
14. Paulson, J. F., Dale, F., and Studniarz, S. A., "Ion-Neutral Reactions with a Time-of-Flight Double Mass Spectrometer," International Journal of Mass Spectrometry and Ion Physics, Vol. 5, pp. 113-126, 1970.
15. Amme, R. C. and Hayden, H. C., "Ion-Beam Excitation Effects on the Single Charge Transfer Between Argon and Nitrogen," Journal of Chemical Physics, Vol. 42, pp. 2011-2015, 1965.
16. Futrell, J. H. (Ed.), Gaseous Ion Chemistry and Mass Spectrometry, Wiley, New York, 1986.
17. Douglas, D. J., "Mechanism of the Collision-Induced Dissociation of Polyatomic Ions Studied by Triple Quadrupole Mass-Spectrometry," Journal of Physical Chemistry, Vol. 86, pp. 185-191, 1982.
18. Dawson, P. H. and Douglas, D. J., "Collisionally Activated Dissociation of Low Kinetic Energy Ions," Tandem Mass Spectrometry, McLafferty, F. W. (Ed.), pp. 125-148, Wiley, New York, 1983.
19. Dawson, P. H., "The Collision-Induced Dissociation of Protonated Water Clusters Studied Using a Triple Quadrupole," International Journal of Mass Spectrometry and Ion Processes, Vol. 43, pp. 195-209, 1982.
20. Dawson, P. H. and Douglas, D. J., "Studies of the Mechanism of Collision-Induced Dissociation at Low Energies Using a Triple Quadrupole," International Journal of Mass Spectrometry and Ion Processes, Vol. 47, pp. 121-124, 1983.

21. Dawson, P. H. and Sun, W. F., "Comparison of Low-Energy Collisionally Induced Dissociation of n-Butylbenzene Ions with Photodissociation," International Journal of Mass Spectrometry and Ion Processes, Vol. 44, pp. 51-59, 1982.
22. Dawson, P. H., "A Study of the Collision-Induced Dissociation of $C_2H_5OH_2^+$ Using Various Target Gases," International Journal of Mass Spectrometry and Ion Processes, Vol. 50, pp. 287-297, 1983.
23. Wright, L. G., McLuckey, S. A., Cooks, R. G., and Wood, K. V., "Relative Gas-Phase Acidities from Triple Quadrupole Mass Spectrometers," International Journal of Mass Spectrometry and Ion Processes, Vol. 42, pp. 115-124, 1982.
24. McLuckey, S. A., Cooks, R. G., and Fulford J. E., "Gas-Phase Thermochemical Information from Triple Quadrupole Mass Spectrometers - Relative Proton Affinities of Amines," International Journal of Mass Spectrometry and Ion Processes, Vol. 52, pp. 165-174, 1983.
25. Boyd, R. K., Bott, P. A., Beynon, J. H., Harvan, D. J., and Hass, J. R., "Collision-Induced Dissociations of Ions from Zero to 4 keV Translational Energy in a Single Apparatus," International Journal of Mass Spectrometry and Ion Processes, Vol. 66, pp. 253-270, 1985.
26. Dass, C., Peake, D. A., and Gross, M. L., "Structures of Gas-Phase C_5H_8 Radical Cations - A Collisional Ionization Study," Organic Mass Spectrometry, Vol. 21, pp. 741-746, 1986.
27. Curtis, J. M., Brenton, A. G., Beynon, J. H., and Boyd, R. K., "A Comparison of 3 Experimental Techniques for Ion Structure Studies via Collision-Induced Reactions - The $[C_5H_8]^+$ Example," Organic Mass Spectrometry, Vol. 22, pp. 779-789, 1987.
28. Dawson, P. H. and Sun, W. F., "Dissociation of the Benzene Ion by Low-Energy Collisions," International Journal of Mass Spectrometry and Ion Processes, Vol. 70, pp. 97-107, 1986.
29. Dawson, P. H., "Low-Energy Collision-Activated Dissociation of n-Butylbenzene - Effect of the Electron Energy Used During Parent Ion Formation," International Journal of Mass Spectrometry and Ion Processes, Vol. 63, pp. 339-341, 1985.
30. Griffiths, I. W., Mukhtar, E. S., March, R. E., Harris, F. M., and Beynon, J. H., "Comparison of Photo-Excitation of Ions and Collisional Excitation Using Gases," International

Journal of Mass Spectrometry and Ion Processes, Vol. 39, pp. 125-132, 1981.

31. Levine, R. D. and Bernstein, R. B., Molecular Reaction Dynamics, Oxford University Press, New York, 1987.
32. Boyd, R. K., Kingston, E. E., Brenton, A. G., and Beynon, J. H., "Angle-Dependence of Ion Kinetic-Energy Spectra Obtained by Using Mass Spectrometers .1. Theoretical Consequences of Conservation Laws for Collisions," Proceedings of the Royal Society of London, Series A - Mathematical and Physical Sciences, Vol. 392, pp. 59-88, 1984.
33. Singh, S., Harris, F. M., Boyd, R. K., and Beynon, J. H., "The Variation of Translational Energy Release in Collision-Induced Dissociations of Polyatomic Ions with Initial Kinetic-Energy and with Observation Angle .1. Theoretical Considerations," International Journal of Mass Spectrometry and Ion Processes, Vol. 66, pp. 131-149, 1985.
34. Herman, Z., Futrell, J. H., and Friedrich, B. A., "Beam Scattering Study of the Collision-Induced Dissociation of Polyatomic Ions CH_4^+ AND C_3H_8^+ at eV Collision Energies," International Journal of Mass Spectrometry and Ion Processes, Vol. 58, pp. 181-199, 1984.
35. Futrell, J. H., "Newton Diagrams for CAD Processes," Unpublished Data, 1987.
36. Davidson, W. R., "Ion Chemistry of $\text{C}_4\text{H}_8\text{O}^+$," Unpublished Data, 1981.
37. Ausloos, P. J. and Lias S. G., "Discrimination of C_3H_3^+ Structures on the Basis of Chemical Reactivity," Journal of the American Chemical Society, Vol. 103, pp. 6505-6507, 1981.
38. Smyth, K. C., Lias S. G., and Ausloos, P., "The Ion-Molecule Chemistry of C_3H_3^+ and the Implications for Soot Formation," Combustion Science and Technology, Vol. 28, pp. 147-154, 1982.
39. Ozturk, F., Baykut, G., Moini, M., and Eyler, J. R., "Reactions of C_3H_3^+ with Acetylene and Diacetylene in the Gas Phase," Journal of Physical Chemistry, Vol. 91, pp. 4360-4364, 1987.
40. Jackson, J. A. A., Lias S. G., and Ausloos, P., "Ion-Cyclotron Resonance Study of Structures of C_7H_7^+ Ions," Journal of the American Chemical Society, Vol. 99, pp. 7515-7521, 1977.

41. Shold, D.M. and Ausloos, P., "Structures of Butyl Ions Formed by Electron-Impact Ionization of Isomeric Butyl Halides and Alkanes," Journal of the American Chemical Society, Vol. 100, pp. 7915-7919, 1978.
42. Martinez, R.I. and Ganguli, B., "Reaction-Induced Mass Discrimination in XQQ Instruments: Absolute Cross Sections for $N_2^+ + SF_6 \rightarrow N_2 + SF_6^+$ (x=1-5)," Rapid Communications in Mass Spectrometry, Vol. 2, pp. 41-46, 1988.
43. Martinez, R.I. and Dheandhanoo, S., "Validation of Absolute Target Thickness Calibration in a QQQ Instrument by Measuring Absolute Total Cross-Sections of $Ne^+(Ne, Ne)Ne^+$," International Journal of Mass Spectrometry and Ion Processes, Vol. 74, pp. 241-250, 1986.
44. Martinez, R.I. and Dheandhanoo, S., "Instrument-Independent CAD Spectral Databases: Absolute Cross-Section Measurements in QQQ Instruments," Journal of Research of the National Bureau of Standards, Vol. 92, pp. 229-237, 1987.
45. Martinez, R.I. and Dheandhanoo, S., "Absolute Cross-Section Measurements in XQQ Instruments: $Ar^+ + N_2 \rightarrow Ar + N_2^+$," International Journal of Mass Spectrometry and Ion Processes, Vol. 84, pp. 1-16, 1988.
46. Martinez, R.I. and Ganguli, B., "Adduct Formation by RCO^+ ," Unpublished Data, 1987.
47. Martinez, R.I., "The NBS Triple Quadrupole Tandem Mass Spectrometer," Review of Scientific Instruments, Vol. 58, pp. 1702-1705, 1987.
48. Louris, J.N., Cooks, R.G., Syka, J.E.P., Kelley, P.E., Stafford, G.C., and Todd, J.F.J., "Instrumentation, Applications, and Energy Deposition in Quadrupole Ion-Trap Tandem Mass-Spectrometry," Analytical Chemistry, Vol. 59, pp. 1677-1685, 1987.
49. Dawson, P.H., "Quadrupole Mass Analyzers - Performance, Design and Some Recent Applications," Mass Spectrometry Reviews, Vol. 5, pp. 1-37, 1986.
50. Enke, C.G., Wade, A.P., Palmer, P.T., and Hart, K.J., "Solving the MS-MS Puzzle: Strategies for Automated Structure Elucidation," Analytical Chemistry, Vol. 59, pp. 1363A-1371A, 1987.

- APPENDIX A
ASMS WORKSHOP REPORT

This appendix contains a copy of the report on the Workshop entitled, "MS/MS CAD Database: Instrument Design and Operation Apposite to CAD Dynamics". It was published on pages 1175-1176 of the proceedings of the 35th ASMS Conference on Mass Spectrometry and Allied Topics held May 24-29, 1987 in Denver, CO. This Workshop was organized by the author to try to reach a consensus among the participants as to the needs of the analytical community in re a MS/MS CAD database.

WORKSHOP

MS/MS CAD Database: Instrument Design and Operation Apposite to CAD Dynamics

Organizers: Richard I. Martinez (NBS) and R. Graham Cooks (Purdue U.)

(Attendance: ca. 180)

The purpose of this Workshop was to examine options for working toward a practical, standardized CAD spectral database for XQQ instruments (QQQ, BEQQ, etc.), and to discuss technical details of instrument design and/or operation essential to the successful development of such a database.

To provide a focus for the Workshop discussion, R.I. Martinez (NBS) presented an overview of published works which indicated that very different CAD spectra are observed for the same molecule on different QQQ instruments; i.e., the relative intensities measured in different QQQ instruments for any one pair of progeny ions differed by factors ranging into the hundreds, even though the same nominal operating conditions were supposedly used in each of the QQQ instruments. This suggests that current instrument designs and/or the choice of parameter settings provide a distorted view of the molecular dynamics of the CAD process (because of scattering losses due to poor ion containment within Q2, fringing fields between Q2/Q3, etc.). Hence, one observes instrument-DEPENDENT CAD spectra. He suggested that one could probably measure instrument-INDEPENDENT CAD spectra under kinetically-correct operating conditions. Workshop participants who use XQQ instruments agreed to participate in the NBS Round-Robin to provide a zeroth order assessment of which instrument designs are kinetically well behaved.

The following report is a summary of written comments submitted by the following participants:

R.K. Boyd (NRC, Canada); R.G. Cooks (Purdue U.); C.G. Enke (Michigan State U.); J. Fulford (SCIEX); J.H. Futrell (U. of Delaware); F. deMaack (Nermag); R.I. Martinez (NBS); F.W. McLafferty (Cornell U.); J.J. Monaghan (ICI); T.H. Pritchett (EPA); J.A.G. Roach (FDA); R. Schaeffer, S. Dheandhanoo, and S. Ketkar (EXTREL); A.E. Schoen (Finnigan); R.A. Yost, J.V. Johnson, and M. Hall (U. of Florida).

The key MS/MS parameters which can cause the relative intensities measured in different QQQ instruments for various progeny ions to differ significantly are:

- (1) the number of collisions undergone by a "parent" ion within Q2, a parameter usually characterized in terms of "target thickness" [(actual path length traversed by the ion in its oscillatory trajectory through the gas target) x (effective number density of the CAD target gas)], and the type of target gas (influences the extent of energy transfer) ;
- (2) the duration of the interaction between the "parent" ion and the target gas, which is determined by the collision energy for "parent" ions entering Q2;
- (3) the energy level of the analyzing quadrupole Q3 relative to that of Q2 which, because of the translational energy distribution of the "progeny" fragment ions, determines whether or not some progeny ions can enter Q3;
- (4) the Mathieu parameter q_2 (rf voltage of Q2) and restrictive interquadrupole apertures of diameter $< 1.4 r_0$, because of mass-dependent focusing effects which determine how effectively parent/daughter ions can be contained within Q2 for emittance (transmission) into Q3; and
- (5) the type of detector used [Daly detector, Channeltron (with or without conversion dynode), etc.] because of differences in mass-dependent conversion gain.

When probed with crossed-beam apparatus, the reaction dynamics of the CAD process are found to be dependent on the internal energy, collision energy, choice of collision gas (deposited energy), scattering angle, and energy of the product ions. Hence, unless the dynamics are taken into account, results in XQQ instruments will be highly instrument dependent, even though reproducible conditions can be established for analytical purposes (with few exceptions, measurements for any given ion within any one XQQ instrument exhibit long-term (9-month interval) reproducibility (precision) to within $\pm 10\%$; one lab reported this precision for 3 different XQQ instruments (QQQ, BEQQ, EBQQ)).

One example was cited to emphasize the need for proper accounting of CAD dynamics in XQQ instruments: for perfluorotributylamine, the relationship $E_{\text{daughter}} = (m_{\text{daughter}}/M_{\text{parent}})^2 E_{\text{parent}}$, between the kinetic energy of the m/z 264 fragment ion (E_{daughter}) and that of the m/z 414 "parent" ion (E_{parent}), changes from $n=1$ to $n=2$ as the Ar gas target thickness is increased; hence, the choice of Q3 pole bias (rod offset) and target thickness will significantly affect the intensity measured for the m/z 264 fragment ion relative to that of other fragment ions.

Major classes of MS/MS experiments: (i) Mixture Analysis [quantitation with or without prior separation (speciation)] and (ii) Structure Elucidation ["isolated" neat compound (prior separation)]. For (i), precision within any one XQQ instrument is critical, and goal is to maximize sensitivity for characteristic daughter ions; need different "standardized" conditions for different substructure classes to compensate for differences in CAD dynamics. For (ii), goal is to maximize number of structurally-significant daughter ions. For both (i) and (ii) it would be very helpful to identify each MS/MS peak according to the collision energy and target thickness required to produce it; this would provide the input necessary for an intelligent program to qualitatively predict a spectrum (cf. presence/absence algorithms (see (b) below)).

For the identification of unknowns, some Government agencies are required by statute to match the spectrum of an unknown to that of a pure standard sample or to a "standard spectral library", following strict criteria for matching the relative ion intensities [presence/absence algorithms (see (b) below) for daughter ions would not suffice for this type of work]. Hence, such agencies need standardized operating conditions and a standard reference library (database) for CAD spectra.

A proposal was made that if all manufacturers were to fully characterize their instruments with respect to the key MS/MS parameters, it may become possible to obtain correction factors with which each type of instrument could be adjusted (following some protocol) to give the same CAD spectra within reasonable limits. If such an approach were to succeed, it might resolve statutory problems faced by Government agencies which use a variety of XQQ instruments from different manufacturers.

Summary of some of the proposals made for conceptually-different CAD databases (symbols designate how each type of proposed database can potentially be utilized: EY (EN)= can (cannot) elucidate structure of unknown compound not included in database; QY (QN)= can (cannot) quantitate unknown compound not included in database):

- (a) EY/QY- Kinetically-correct (single-collision conditions) CAD database of absolute cross sections for the CAD of ionic substructures measured under standardized operating conditions (may have to use different standardized conditions for different substructure classes to compensate for differences in CAD dynamics)
- (b) EY/QN- Collect complete MS/MS "map" (all the daughters of all the parents) under single-collision conditions and relatively high collision energy; database based on the presence (bona fide neutral loss) or absence of ion signal at particular combinations of parent and daughter masses (correspond to specific ion substructures); spectrum matching algorithms that weight the presence/absence of peaks more and the relative ion abundances less yield better daughter spectrum matches than the algorithms borrowed from matching normal mass spectra.
- (c) EN/QN- Analytically useful (but not necessarily kinetically-correct) reference spectra to be used within either one single XQQ instrument or within many XQQ instruments of the same model (one manufacturer) operated under identical, standardized conditions.
- (d) EN/QN- Based on current knowledge, prescribe pseudo-standard conditions (e.g., 70 eV for electron impact ionization), and collect a very large number of contributed CAD "reference" spectra (masses and abundances) from all types of XQQ instruments; statistical analysis will provide a basis for a search algorithm for structure elucidation ("quality index", etc.), and for fine-tuning the standardization rules as our knowledge grows.

HQ Dept of the Army-COE/DAEN-RDM
20 Massachusetts Ave, NW
Washington DC 20314-100

89-12

Commander
US Army Construction Engineering
Research Laboratory
PO Box 4005
Champaign IL 61820-1305

Commander
US Army Medical Bioengineering Research
and Development Laboratory
Attn: SGRD-UBG
Fort Detrick
Frederick MD 21701

Commander
US Army Engineers
Environmental Engineering Division
Waterways Experiment Station
Vicksburg MS 39180

Dept of the Army
Cold Regions Research and Engineering Laboratory
Hanover NH 03755-1290

Commander
US Army Environmental Hygiene Agency
Attn: HSHD-E
Aberdeen Proving Grounds MD 21010-5422

Commander
US Army Toxic and Hazardous Materials Agency
Attn: AMXTH-TE
Aberdeen Proving Grounds MD 21010-505401

Naval Civil Engineering Laboratory
Code L70PN
Port Hueneme CA 93043

Naval Civil Engineering Laboratory
Code L70PMP
Port Hueneme CA 93043

Naval Civil Engineering Laboratory
Code L71
Port Hueneme CA 93043

Naval Facilities Engineering
Command Headquarters
Code 032P
200 Stoval Street
Alexandria VA 22332

Naval Facilities Engineering
Command Headquarters
Code 1121
200 Stovall Street
Alexandria VA 22332

Northern Division
Naval Facilities Engineering Command
Code 114
Philadelphia PA 19112

Chesapeake Division
Naval Facilities Engineering Command
Code 114
Bldg 212, Washington Navy Yard
Washington DC 20374

Atlantic Division
Naval Facilities Engineering Command
Code 114
Norfolk VA 23511

Southern Division
Naval Facilities Engineering Command
Code 114
PO Box 10068
Charleston SC 29411

Western Division
Naval Facilities Engineering Command
Code 114
PO Box 727
San Bruno CA 94066

Pacific Division
Naval Facilities Engineering Command
Code 114
Pearl Harbor HI 96860

Naval Energy and Environmental Support
Activity
Code 112
Port Hueneme CA 93043

Defense Logistics Agency
DLA/WS/DEPO
Cameron Station
Alexandria VA 22304-6100

Commandant (G-WP-3)
U.S. Coast Guard
2100 2nd St. S.W.
Washington DC 20593

Defense Revitalization and Marketing
Service
Chief, Technical Support Division
Environmental Protection Directorate
Federal Center
Battle Creek MI 49017

Chief of Naval Operations
OP44
Pentagon
Washington DC 20301

Chief of Naval Operations
OP45
Washington DC 20350-2000

National Center for Groundwater Research
Department of Environmental Science and
Engineering
Rice University
Houston TX 77001

National Center for Groundwater Research
School of Civil Engineering and Environmental
Science
University of Oklahoma
Norman Oklahoma 73019

National Center for Groundwater Research
Dean of the Graduate School
Oklahoma State University
Stillwater Oklahoma 74074

Hazardous Waste Research Center
3418 CEBA
Louisiana State University
Baton Rouge LA 70803-6421

U.S. Environmental Protection Agency
Environmental Monitoring Systems
Laboratory/LV
PO Box 15027
Las Vegas NV 89114

U.S. Environmental Protection Agency
Environmental Monitoring Systems Laboratory/
RTP
Research Triangle Park NC 27711

U.S. Environmental Protection Agency
Environmental Research Laboratory/
ATH
College Station Road
Athens GA 30613

U.S. Environmental Protection Agency
Environmental Research Laboratory/GB
Sabine Island
Gulf Breeze FL 32561

U.S. Environmental Protection Agency
Hazardous Waste Engineering Research
Laboratory/In Situ Technology Branch
Cincinnati OH 45268

U.S. Environmental Protection Agency
Water Engineering Research
Laboratory/SITE Program
Cincinnati OH 45268

U.S. Environmental Protection Agency
Office of Environmental Engineering and
Technology/HQ
(RD-681)
Washington DC 20460

U.S. Environmental Protection Agency
Robert S. Kerr Environmental Research
Laboratory/(Dr Wilson)
PO Box 1198
Ada OK 74820

DTIC/DDA-2
Cameron Station
Alexandria VA 22304

HQ Aeronautical Systems Division
ASD/PMD
Wright Patterson AFB OH 45433-6503

USAFOEHL/CC
Brooks AFB TX 78235-5000

HQ USAF/LEEV
Bolling AFB DC 20332-5000

HQ USAF/DEEVO
Bolling AFB DC 20332-5000

AUL/LSE 71-249
Maxwell AFB AL 36112-5000

SAF/RQ
Washington DC 20330

USAF OEHL/TS
Brooks AFB TX 78235-5000

OASD(MI&L) I/EP
Office of the Assistant Secretary
of Defense
Assistant to the Director of
Environmental Policy
The Pentagon, Room 3D833
Washington DC 20301-4000

OUSDRE/R&AT
Acting Under Secretary of Defense for
Research & Advanced Technology
The Pentagon, Room 3E114
Washington DC 20301-3080

HQ USAF/SGPA
Bolling AFB DC 20332-5078

HQ AAC/SGPB
Elmendorf AFB AK 99506-5300

HQ AAC/DEV
Elmendorf AFB AK 99506-5000

HQ ATC/SGPAB
Randolph AFB TX 78150-5001

HQ ATC/DEV
Randolph AFB TX 78150-5000

HQ MAC/SGPB
Scott AFB IL 62225-5001

HQ MAC/DEV
Scott AFB IL 62225-5000

HQ PACAF/SGPA
Hickam AFB HI 96853-5001

HQ PACAF/DEV
Hickam AFB HI 96853-5000

HQ AFLC/SGPB
Wright-Patterson AFB OH 45433-5001

HQ AFLC/DEV
Wright-Patterson AFB OH 45433-5000

HQ AFSC/SGPB
Andrews AFB DC 20334-5000

HQ AFSS/DEV
Andrews AFB DC 20334-5000

HQ AFSC/~~SGB~~
Andrews AFB DC 20334-5000

HQ AFSC/~~DLW~~
Andrews AFB DC 20334-5000

HQ SAC/~~SGPB~~
Offutt AFB NE 68113-5001

HQ SAC/~~DEV~~
Offutt AFB NE 68113-5000

HQ AFSPACECOM/~~DEPV~~
Peterson AFB CO 80194

HQ AFSPACECOM/~~SGB~~
Peterson AFB CO 80194

Space Division
SD/~~DEV~~
PO Box 92960
Worldway Postal Center
Los Angeles AFS CA 90009-2960

HQ TAC/~~SGPB~~
Langley AFB VA 23665-5001

HQ TAC/~~DEV~~
Langley AFB VA 23665-5000

HQ USAFE/~~SGPA~~
APO New York 09012

HQ USAFE/~~DEV~~
APO New York 09012

AF Regional Civil Engineer/
WR/~~ROV~~
630 Sansome Street, Room 1316
San Francisco CA 94111

AF Regional Civil Engineer/
CR/~~ROV~~
1114 Commerce Street
Dallas TX 75242

AF Regional Civil Engineer/
ER/~~ROV~~
30 Pryor Street, SW
526 Title Building
Atlanta GA 30303

AFIT/~~DE~~
Wright-Patterson AFB OH 45433

AFIT/DEM
Wright-Patterson AFB OH 45433

~~Dr. Wayne Hansen
Environmental Science Group
Los Alamos National Laboratory
MSP 373
Los Alamos NM 87545~~

~~Dr. Jim Gossett
Dept of Environmental Engineering
Cornell University
Hollister Hall
Ithaca NY 14853~~

HQ AFCC/DEV
Scott AFB IL 62225-5000

HQ AFRES/DEV
Robins AFB GA 31098-5000

HQ AFRES/SGPB
Robins AFB GA 31098-5000

HQ AU/DE
Maxwell AFB AL 36112-5000

HQ ESC/DE
San Antonio TX 78243-5000

ANGSC/SGP
Andrews AFB MD 20331-5000

ANGSC/DEV
Washington DC 20310-5000

HQ USAFA/DE
USAFA CO 80840-5000

HQ USAFA/DFCE
USAFA CO 80840-5000

Engelhard Corporation
Menlo Park, CA-40
Edison, NJ 08818
Attn: Mr L. Winja

EPA Air and Energy Engineering
Research Laboratory
Research Triangle Pk NC 27711
Attn: ~~Dr B. Tichenor~~/MDF-61
Mr C. Nunez

(5 copies)

Chemical Engineering Department - 2 copies
University of Akron
Akron, Ohio 44325
Attn Dr Howard Greene